fibers

MDPI

Article

Comparative Study of Atmosphere Effect on Wood Torrefaction

Rafael Lopes Quirino [1,*], Larissa Richa [2], Anelie Petrissans [2], Priscila Rios Teixeira [2], George Durrell [1], Allen Hulette [1], Baptiste Colin [2] and Mathieu Petrissans [2]

[1] Chemistry Department, Georgia Southern University, Statesboro, GA 30460, USA
[2] INRAE, LERMAB, Université de Lorraine, F-88000 Epinal, France
* Correspondence: rquirino@georgiasouthern.edu

Abstract: Climate change, biomass utilization, and bioenergy recovery are among the biggest current global concerns. Wood is considered an environmentally benign material. Nevertheless, it must be processed for desired applications. Upon thermal treatment ranging from 180 °C to 280 °C, under low oxygen concentrations, wood becomes a material with improved dimensional stability, resistance to fungal attacks, grindability, hydrophobicity, and storage stability. Several strategies for wood treatment have been investigated over the course of the past decades, including the use of steam, nitrogen, smoke, vacuum, water, and hot oil. The goal of this work is to investigate the influence of pressure and atmosphere on the torrefaction of poplar. Through a systematic analysis of poplar wood samples treated under reduced pressures and different atmospheres, while keeping the same heating profile, it was possible to establish that changes observed for mass loss, color change, wood composition (via TGA/DTG analysis), functional groups (via FTIR), elemental analysis, and X-ray diffractograms relate directly to known reaction pathways occurring during torrefaction. Changes observed under reduced pressures have been associated with the relative concentration of oxygen in the reaction atmosphere and to the reduced diffusion times experienced by reactive by-products during the treatment. Conversely, extended diffusion times resulted in more significant changes for reactions carried out under N_2, water vapor, and air.

Keywords: torrefaction; pressure; atmospheres; poplar; materials

Citation: Quirino, R.L.; Richa, L.; Petrissans, A.; Teixeira, P.R.; Durrell, G.; Hulette, A.; Colin, B.; Petrissans, M. Comparative Study of Atmosphere Effect on Wood Torrefaction. *Fibers* **2023**, *11*, 27. https://doi.org/10.3390/fib11030027

Academic Editor: Vincenzo Fiore

Received: 26 January 2023
Revised: 24 February 2023
Accepted: 28 February 2023
Published: 7 March 2023

1. Introduction

Despite its abundant use in construction, the exposure of untreated wood to the elements results in degradation, primarily promoted by fungal attacks. Wood treatment by torrefaction at 180–240 °C is considered a low environmental impact process, without the addition of chemicals. It is therefore viewed as a promising alternative to chemical treatments for the enhancement of the local biomass, with improvement of stability [1,2], durability [3,4], and its economic potential. Wood torrefaction is becoming increasingly popular in Europe. Despite the latest progress, there is still a lack of process control and property uniformity of torrefied samples [1]. During wood thermal treatments, even for well-known wood species, cracking and delamination are often observed due to uneven treatment across the heated material. Torrefaction conditions are usually established empirically, without a full comprehension of individual factors, such as reaction atmosphere and pressure.

Torrefaction increases hydrophobicity [5], darkness [6], and stability, and decreases the high heating value (HHV) of woody biomass [7]. Torrefaction is often applied to wood boards. Chemically, the process consists of crosslinking and condensation when higher temperatures are employed, while extensive bond scission prevails at lower temperatures [8]. Hemicelluloses are completely degraded during severe torrefaction [9], with a higher susceptibility for hemicelluloses from hardwood [10]. A slight increase in cellulose crystallinity is observed when torrefaction is carried-out at low temperatures and sharply decreases at high temperatures, revealing a competitive behavior between the degradation

of crystalline *versus* amorphous cellulose [11]. The main wood torrefaction products are solids, condensables, and non-condensable volatiles [12].

Despite several literature reports [13,14], the fundamentals of the chemical transformations during torrefaction under different conditions are not yet fully elucidated. Hydrophobicity has been studied for torrefaction carried out at temperatures higher than 240 °C in the presence of water [15]. In a different study, lignin derivatives have been detected on the surface of pine wood samples treated at 225–350 °C [13].

Several studies have evaluated the torrefaction products obtained under inert (N_2, vacuum) and oxidative (O_2, CO_2, steam, air) atmospheres, with scattered results reported. Because torrefaction is highly dependent on the biomass used and the temperatures employed, it is exceedingly difficult to compare results reported in different published articles focusing on various biomasses and adopting a multitude of reaction conditions. In many reports, it has been mentioned that the atmosphere is significantly less impactful on torrefaction products than temperature, and for temperatures lower than 240 °C, the properties of biomass torrefied under different atmospheres is not statistically different [12,16–22]. Additionally, there are many accounts of lower ash content in detriment of an increase in gas products yielded when CO_2 is used during torrefaction [17–22], as well as an increase in fixed carbon content [23].

For experiments evaluating the effect of O_2 during torrefaction, it has been reported that increasing O_2 concentrations result in lower degradation temperatures to achieve a desired mass loss, more extensive degradation rates, better product properties [18,24,25], and lower solid yields in detriment of liquid products [26,27]. Similar trends have been observed when steam is employed [28,29]. For experiments carried out under a vacuum, it has been shown that products with a larger higher heat value (HHV) are obtained due to better diffusion of lower molecular weight degradation fragments and products [12], and that torrefaction is dominated by surface oxidation [30].

Herein, a systematic evaluation of the atmosphere effect on poplar wood torrefaction under consistent and comparable heating conditions is proposed. The atmospheres evaluated in this study are N_2, air, water vapor, and reduced pressure (200 hPa, 300 hPa, 500 hPa, and 600 hPa, resulting in O_2 concentrations of 4%, 6%, 8%, and 10%, respectively). The careful investigation of the atmosphere effect on torrefaction at a molecular level gives an improved understanding of the chemical transformations that occur, allowing for specific parameter controls in order to obtain products with desired properties. All torrefied products were analyzed with respect to their compositional evolution by colorimetric measurement, thermogravimetric analysis (TGA), elemental analysis, Fourier-transform infrared spectroscopy (FTIR), and X-ray diffraction (XRD). The results indicate that steam and higher concentrations of Oxygen result in a more significant change of the torrefaction process.

2. Material and Methods

2.1. Materials and Thermal Treatment Conditions

Poplar (*Populus nigra*), with an average density of 400–500 kg m^{-3}, was used in this study. The samples were cut from the same board according to the fiber orientation in specimens of 20 mm^3 × 100 mm^3 × 300 mm^3 (tangential × radial × longitudinal) for experiments carried out in a conductive oven, and of 20 mm^3 × 70 mm^3 × 600 mm^3 (tangential × radial × longitudinal) for experiments carried out in a convective oven. All samples were stored at 103 °C prior to the experiments described herein.

Industrially, the production of thermally modified wood is performed at 200–240 °C, until reaching 8–10 wt.% of mass loss [31]. For this reason, the heat treatment in this study was conducted at 235 °C. The temperature was initially increased to 105 °C at 0.2 °C min^{-1} followed by a 30 min isothermal to remove any moisture adsorbed onto the samples and the initial mass was precisely record. Subsequently, the temperature is increased to 170 °C at 0.2 °C min^{-1} and held for 30 min. Industrially, this stage avoids cracking [32]. Finally,

the temperature was increased to 235 °C at 0.2 °C min^{-1} and maintained for 1000 min. Mass loss (*ML*) is calculated as follows:

$$ML\ (\%) = \frac{M_i - M_t}{M_i} \times 100 \quad (1)$$

where M_i corresponds to the anhydrous mass and M_t corresponds to the final mass of the sample.

Experiments in both ovens were performed on two boards simultaneously. The vacuum conductive oven used pressure levels varying from 200 hPa to 600 hPa, with oxygen concentrations of 4%, 6%, 8%, 10%, and 12%.

2.2. Experimental Devices

Reduced pressure treatments were conducted in a conductive oven with pressures in a range of 200–1000 hPa. Pictures of this system are shown in Figure 1**.** The conductive experimental system (Figure 1) is composed of an electrically heated unit, a control unit, and a vacuum pump. Poplar boards are sandwiched between electrically heated metal plates. A total of three samples can be simultaneously treated. Thermocouples were inserted between the metal plates and in direct contact with the sample. A computer with monitoring software controlled and recorded temperature and mass during the process. Instantaneous mass is recorded during the treatment with 1 s intervals and a precision of 1 g.

Figure 1. Conductive vacuum reactor.

Thermal treatments under various atmospheres were conducted in a convective oven (Figure 2). The convective unit is able to evenly treat 10 boards simultaneously. The system can be swept by different pre-heated gases at 30 L min^{-1}. Volatiles, mixed with the sweeping gases, are bubbled through water.

Figure 2. Convective multi atmosphere reactor.

2.3. Characterization

Colorimetric readings were performed with a CR-410 Konica Minolta device [33]. The results reported herein correspond to the average of three readings performed on different locations of each sample. L* represents the black–white axis (where L* = 0 corresponds to total black and L* = 100 corresponds to pure white). a* represents the green–red axis (where positive values correspond to red and values lower than 0 correspond to green), while b* represents the blue–yellow axis (where positive values correspond to yellow and negative values correspond to blue). ΔE^* is expressed by the following equation [33].

$$\Delta E = \sqrt{(L_t^* - L_i^*)^2 + (a_t^* - a_i^*)^2 + (b_t^* - b_i^*)^2} = \sqrt{(\Delta L^*)^2 + (\Delta a^*)^2 + (\Delta b^*)^2} \quad (2)$$

where subscripts "i" and "t" represent raw and treated samples, respectively.

A Q50 thermogravimetric analyzer (TA Instruments, New Castle, DE, USA) was used for all TGA experiments using a platinum pan to determine the pyrolysis characteristics of biomass samples. A sample size of ~5.0 mg was used for TGA experiments, with a N_2 flow of 20 mL min^{-1}. The samples were heated from 50 °C to 105 °C, followed by a 10-min isothermal step. The samples were then heated from 105 °C to 800 °C at 20 °C min^{-1}. The carrier gas was changed to air at 600 °C to clean the pan. The derivative of each TGA curve (DTG) was calculated on Origin 9 and the curves were smoothed using a 10-point average.

FTIR was used to evaluate structure changes in the samples. A Nicolet IS10 spectrometer containing a Germanium 1126 Crystal was used. Sixteen scans were collected per run with a spectral resolution of 4 cm^{-1} in the spectral region of 400–4000 cm^{-1}. FTIR was used to determine how the reaction atmosphere during torrefaction affects six specific bonds, namely C-O-C, C(sp^3)-H, C(sp^2)-H, O-H, C=C, and C-O.

Elemental analysis was conducted on a Flash 2000 Organic Elemental Analyzer with CHNS-O. The results were processed with the software Eager Xperience (EX). Each sample was burned in the furnace for 12 min. EDS experiments were conducted on a JSM-760F Field Emission Scanning Electron Microscope (JEOL, Peabody, MA, USA) equipped with an EDS detector. Grinding greatly affects the topography and morphology of wood samples when observed with SEM; therefore, it is practically impossible to distinguish features that are the result of the thermal treatments applied from the direct physical effect of grinding.

An Empyrean Malvern PANalytical Powder X-ray Diffractometer was used to collect diffraction patterns of all samples with $5° < 2\Theta < 60°$. The output data is the average of 10 diffractograms averaged together. The intensity of the diffraction angle of amorphous cellulose (I_{am}) was determined from the minimum intensity in the 2Θ region of 17.5°–19°. The maximum intensity in the 200 plane (I_{200}) was determined from the maximum intensity in the 2Θ region of 21.5°–23°. The crystallinity index (*CrI*) was calculated according to Equation (3).

$$CrI\ (\%) = \frac{I_{200} - I_{am}}{I_{200}} \times 100 \quad (3)$$

3. Results and Discussion

3.1. ML

Good durability and retention of mechanical properties are achieved with MLs ranging from 10 wt.% to 15 wt.% [34,35]. To verify the requirements for construction and furniture applications, the averaged MLs of all samples are reported in Table 1. All treatment conditions achieve the target degradation level. Experimental mass loss varies between 12.81 wt.% and 16.48 wt.%. No clear trend can be reported between the treatment atmosphere and the global biopolymers' degradation. The investigation of the experiments conducted under reduced pressure shows that even with pressure increasing from 200 hPa to 600 hPa (increasing O_2 concentration), no clear change on the ML is detected. In fact, the influence of pressure on the torrefaction of wood is significantly complex. Pressures of 200–300 hPa extract small volatile molecules from wood's pores and vessels resulting from the degradation of major wood constituents, preventing re-polymerization reactions.

Higher pressure (500–600 hPa) eliminates only smaller fragments and corresponds to a higher oxygen concentration. The competition of these two phenomena significantly modifies the treatment transformation conditions.

Table 1. ML of poplar wood samples for each treatment employed.

Torrefaction Conditions	ML (%)
Reduced pressure experiments	
200 hPa	15.16 ± 0.12
300 hPa	13.44 ± 0.06
400 hPa	13.22 ± 0.41
500 hPa	13.30 ± 0.52
600 hPa	14.24 ± 0.26
Different atmospheres	
N_2	16.48 ± 0.59
Water vapor	14.97 ± 0.98
Air	12.81 ± 0.24

When vacuum and nitrogen treatments are compared, the following speculations could be suggested. Small molecule volatiles, such as acetic acid and furfural produced from hemicelluloses' degradation, catalyze biomass degradation. Torrefaction under reduced pressure rapidly removes volatiles. The higher ML observed under N_2 is possibly the result of an acetic acid by-product in the system. For experiments under air, it was anticipated that the presence of O_2 would promote oxidation of lignin, cellulose, and hemicelluloses, increasing the rate of degradation and ML evolution. The trends observed did not match this expectation. It is worth mentioning that the difference between ML for the different samples is not statistically persuasive given the data dispersion.

3.2. Color Change

Changes in wood color are typically associated with chemical modifications resulting from the action of temperature combined with pressure, moisture, and oxygen in the air. The combination of these factors can create an environment conducive to the depolymerization of cellulose and lignin, resulting in chemical changes in the sample [36]. Figure 3 shows ΔL*, Δa*, and Δb for poplar wood samples treated under reduced pressure at different levels. There is an overall decrease in ΔL* when the pressure during the treatment goes from 200 hPa to 600 hPa. Negative ΔL* (as reported in Figure 3) represents darkening of the thermally treated samples with respect to their untreated counterpart. Although minimal differences are observed for ΔL*, there is an overall tendency of lower ΔL* values for higher pressures utilized during the treatment.

Indeed, when wood is thermally treated under reduced pressure, there is no stream of gas flowing during the experiment, which creates a stale atmosphere at a constant, pre-set pressure. The different levels of reduced pressure utilized during the experiment are obtained by the partial suppression of air inside the reactor. Therefore, increasing pressures represent an increase in the remaining Oxygen and moisture content inside the reactor. It is believed that the residual oxygen in the reactor is responsible for promoting oxidation and degradation of polysaccharides, such as cellulose and hemicelluloses, therefore increasing the relative concentration of lignin left in the treated sample. Due to the natural dark-brown color of lignin, samples that are richer in lignin exhibit a darker color, and are reflected in lower ΔL* values. The removal of oxidized/degraded polysaccharide fragments is facilitated by the reduced pressure. Any gaseous products formed during the experiment are immediately removed by the action of the vacuum pump employed in order to keep a consistent pre-set pressure throughout the experiment. It is therefore logical that darkening increases (lower ΔL* values) for higher pressures employed during experiments conducted under reduced pressure, as observed in Figure 3.

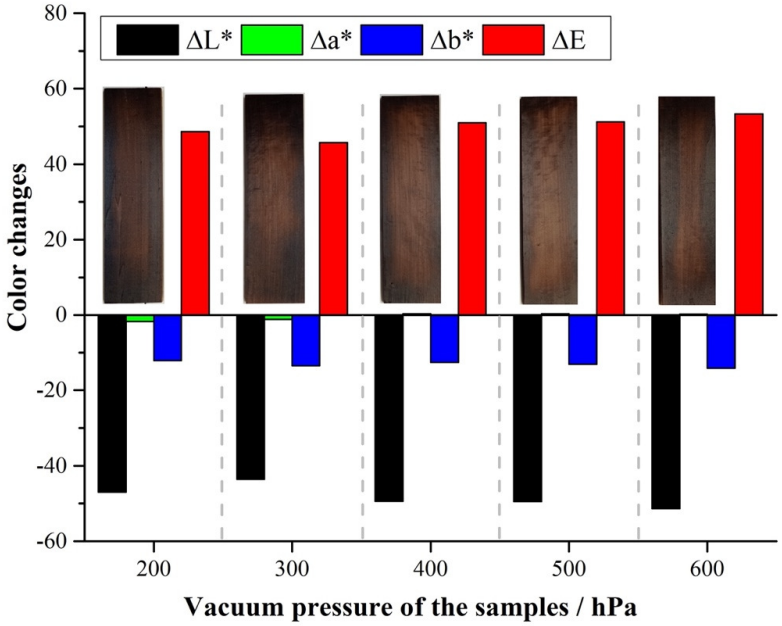

Figure 3. ΔL*, Δa*, Δb*, and ΔE for poplar samples treated under reduced pressure at 200–600 hPa.

Unlike for ΔL*, the different values measured for Δa* (green/red) and Δb* (yellow/blue) aren't statistically different across the samples analyzed (Figure 3), revealing that the main component responsible for the color changes observed is ΔL*. ΔE (Figure 3) increases as pressure increases. From the expression presented in Equation (2), lower ΔL* values lead to higher ΔE numbers. As expected, the trend observed in ΔE (Figure 3) correlates well with the results presented and shows that color change is indeed dominated by ΔL* behavior.

Similarly, when the thermal treatment is conducted under different atmospheres, the color change is dominated by ΔL* behavior, with a lower contribution from Δb*, as observed in Figure 4. The color change results suggest that a more oxidative atmosphere, such as water vapor and air, results in darker samples, corroborating the idea that oxidation/degradation of polysaccharides leads to samples with a higher relative lignin content. Indeed, for torrefaction under a water vapor atmosphere, lower ΔL* and higher ΔE values are obtained than for samples treated under an unreactive N_2 atmosphere (Figure 4). The color change is significantly more pronounced when the treatment is carried out under the highly oxidative air atmosphere (Figure 4). Indeed, chromophores, such as colored quinoids, can be generated under oxidizing conditions and can catalyze depolymerization and degradation [37]. The darkening of wood under heat treatment has also been attributed to the decrease of hemicelluloses [38]. Shao-Ni Sun et al. have suggested that, upon thermal treatment, the β-O-4′ bonds in lignin convert into ketones [39].

3.3. Thermogravimetric Analysis

With the objective of investigating the effect of different atmospheres on the torrefaction of poplar wood and the reaction pathways involved in the process, a thermogravimetric analysis (TGA) and its derivative (DTG) have been performed. TGA and DTG results of samples treated in a conductive vacuum oven and a convective oven with different atmospheres are shown in Figures 5 and 6, respectively. The TGA curves (Figures 5a and 6a) reveal that degradation of poplar wood happens primarily at 200–400 °C. Figures 5a and 6a show the differences of the degradation rate with the different atmospheres used. Untreated poplar degrades much faster than the treated samples. That change can be associated with the continuous degradation and removal of volatiles and lower molecular weight (Mw) degradation by-products. For the torrefied samples, these degradation by-products were partially removed during torrefaction, resulting in a decreased weight loss during TGA.

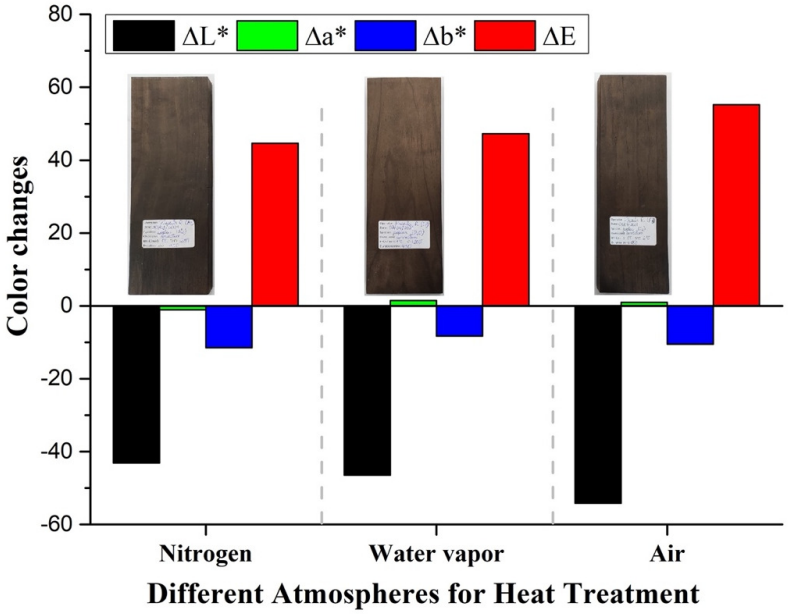

Figure 4. ΔL*, Δa*, and Δb*, and ΔE for samples treated under Nitrogen, water vapor, and air atmospheres.

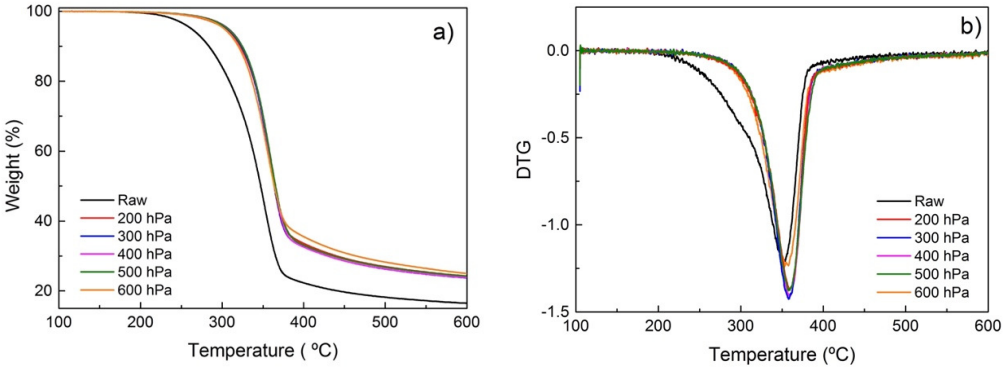

Figure 5. (**a**) TGA and (**b**) DTG for poplar treated at reduced pressures.

As seen in Figure 5a, the TGA profiles of samples treated under reduced pressure are very similar in the 100–600 °C range, with the only noticeable difference being the maximum of the main DTG peak at ~370 °C (Figure 5b), which is associated with cellulose degradation [40]. Aside from the sample treated at 200 hPa, the absolute intensity of the DTG peak maximum is higher when the samples are treated at lower pressures. The breadth of the DTG signal is associated with the relative crystalline cellulose content [41]. At a lower pressure, volatile fragments are more easily removed, leaving behind a material with a higher relative concentration of crystalline cellulose.

For samples treated under different atmospheres, the maximum degradation also occurs between 200 °C and 400 °C (Figure 6a). Interestingly, the sample treated under N_2 exhibits a faster degradation than the one treated under water vapor, while the lowest degradation rate is detected for the sample treated under air. That translates into a shift of the temperature at the DTG maximum. The DTG maximum for samples treated under water vapor and air shifts respectively to 361 °C and 368 °C. The upward shift in the DTG maximum temperature could be rationally explained by the possible repolymerization of oxidized fragments. De-polymerization and re-polymerization are known competing processes during the thermal degradation of ligno-cellulosic biomass [42,43]. Indeed, rationally, under oxidative/reactive atmospheres, it is possible that sample fragments are easily oxidized and re-polymerized, resulting in more stable by-products.

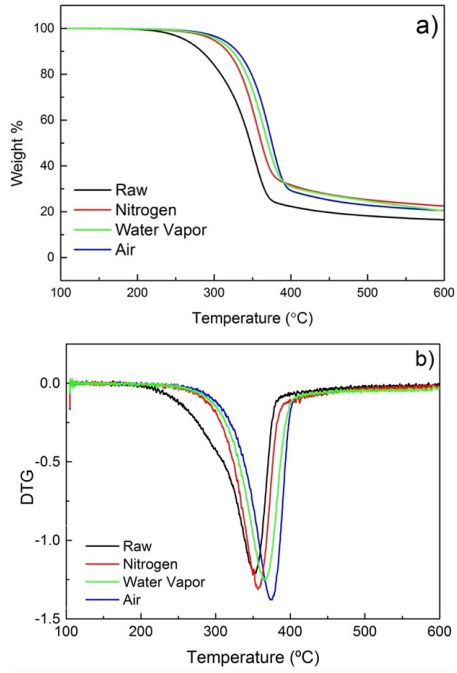

Figure 6. (**a**) TGA and (**b**) DTG for poplar treated under varying atmospheres.

3.4. FTIR

FTIR was used to monitor specific functional groups in heat-treated poplar. Figure 7 shows a section of the FTIR spectrum (4000–3000 cm^{-1}) for wood samples treated under pressures ranging from 200 hPa to 600 hPa. This region specifically includes hydrogen bonded O-H [44]. A pronounced signal at 3370 cm^{-1} can be observed in Figure 7a, attributed to the O-H bond of hydroxyl groups. This signal has a characteristic broad shape due to the intermolecular and intramolecular hydrogen bonds of carbohydrates [45]. The OH signal decreases significantly when comparing the untreated sample and the samples treated at different pressures (Figure 7), indicating that significant degradation of carbohydrates, such as cellulose and hemicelluloses, is achieved under a vacuum. No significant changes in the OH peak are detected for the different pressures used (Figure 7b–f).

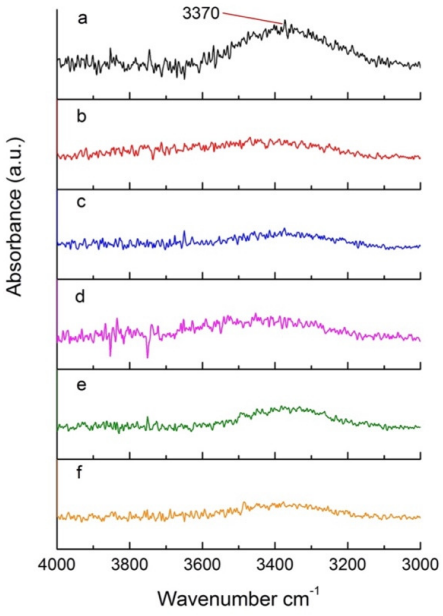

Figure 7. Section of the FTIR spectra of (**a**) untreated poplar and (**b**–**f**) poplar treated at reduced pressures.

Figure 8 shows a section of the FTIR spectrum of poplar wood treated under different pressures. This region contains many bands attributed to different groups from wood components. The signal at 1659 cm^{-1} (Figure 8a) is attributed to conjugated CO in quinines and to carbonyl stretching in hemicelluloses. That signal completely disappears for samples treated under different reduced pressures (Figure 8b–f). This is associated with the deacetylation of hemicelluloses, releasing acetic acid, which catalyzes depolymerization of cellulose through acid hydrolysis [44,46].

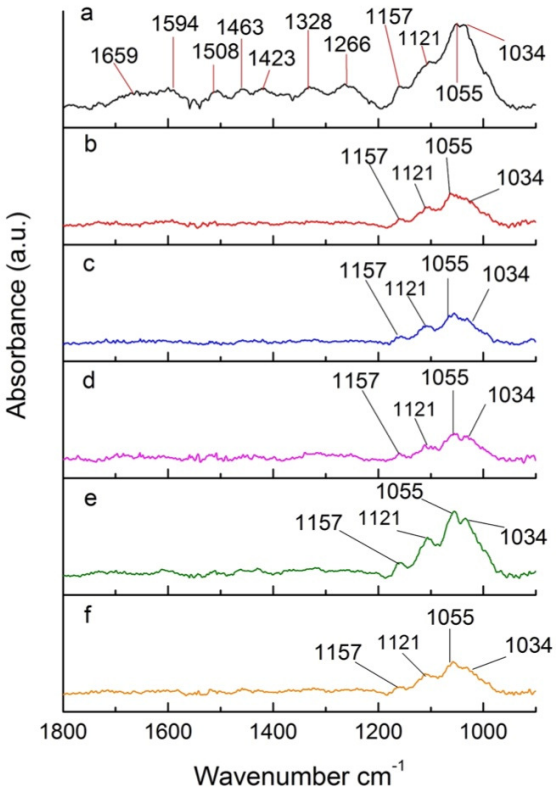

Figure 8. Section of FTIR spectra of (**a**) untreated poplar and (**b**–**f**) poplar treated at reduced pressures.

The bands of 1594 cm^{-1} and 1508 cm^{-1}, referring to the C=C stretching of substituted aromatic rings in lignin [47], also disappear in the spectrum of samples treated under different pressures (Figure 8), indicating that lignin is also degraded during the thermal treatment. Ozlem et al. [46] proposed that the cleavage of carbon chains in lignin is responsible for the absence of the characteristic peak in the spectra of treated poplar [48]. The break down of lignin can also be associated with the disappearance of the bands at 1463 cm^{-1}, 1423 cm^{-1}, and 1382 cm^{-1}, assigned to CH_3 asymmetric stretch, CH_2 scissoring, CO stretch, and CH deformation, respectively [49]. The 1266 cm^{-1} band, which also completely disappears after heat treatment under different pressures, is characteristic of CH bending and CO stretch, demonstrating degradation of lignin and cellulose upon torrefaction at reduced pressures [49].

The bands less affected by oxygen concentration are 1157 cm^{-1}, 1121 cm^{-1}, 1055 cm^{-1}, and 1034 cm^{-1}, associated with COC vibrations in carbohydrates, COH deformation, and CO vibrations in carbohydrates and lignin, respectively [46]. The signals in the 1200–900 cm^{-1} region are associated with xylose [50]. The presence of these signals in all heat-treated samples (Figure 8b–f) indicate that these characteristic groups of cellulose and hemicelluloses are not completely degraded. Interestingly, for the sample treated under a pressure of 500 hPa (approximately 10% oxygen concentration—Figure 8e), there is an increase of the signals at 1200–900 cm^{-1} in comparison to other heat-treated samples (Figure 8b–d,f). Despite the experiments being reproducible, there are few clues that could help explain this behavior. It is possible that a competition between the hydrolysis of

carbohydrates and recondensation of monosaccharides takes place during the thermal treatment. These two processes can be affected by the presence of Oxygen, with recondensation being favored at 500 hPa. Further studies with model compounds could help better elucidate the specific effect of Oxygen concentration on the thermal degradation mechanism of ligno-cellulosic materials.

A different behavior is observed for samples treated in a convection oven under N_2, water vapor, and air (Figure 9). The intensity of the signal at 3370 cm^{-1} visibly decreases for more oxidative atmospheres (Figure 9b–d), such as water vapor and air, with treatment under air exhibiting the lowest intensity for that signal. This indicates that water and Oxygen in the air contribute to the dehydration (loss of O-H) from lignin, cellulose, and hemicelluloses [51]. The peaks at 1800–900 cm^{-1}, primarily associated with the C-O stretch, decrease upon thermal treatment (Figure 9e versus Figure 9f–h), but remain practically unchanged across the different atmospheres used (Figure 9f–h). The heat-catalyzed hydrolysis and the subsequent dehydration of hydrolyzed sugar units from carbohydrates explain the decrease in the CO stretch. This process seems to be primarily controlled by heat and is little affected by the oxidative nature of the atmosphere used.

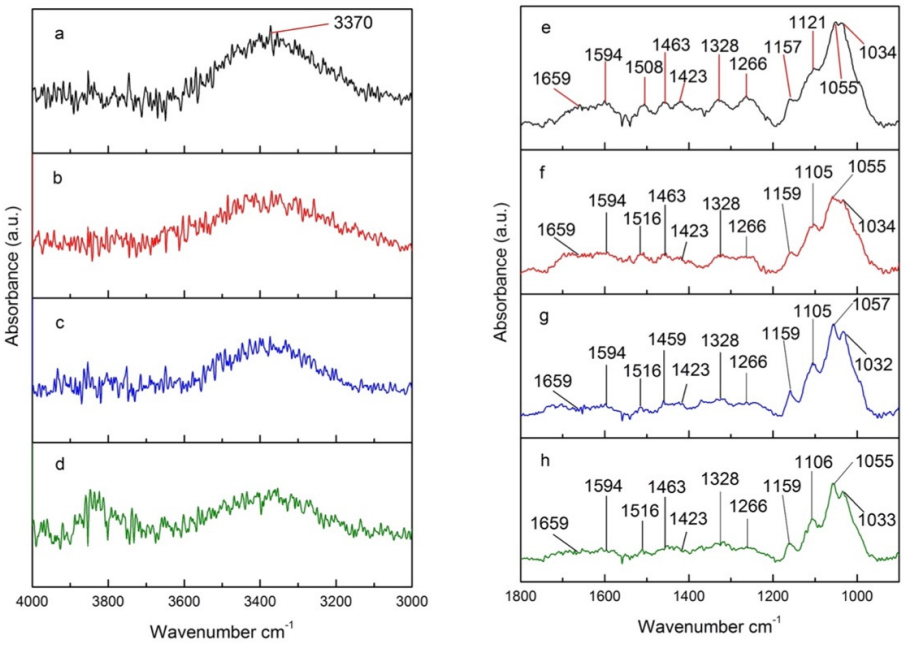

Figure 9. 4000–3000 cm^{-1} section of FTIR spectra of (**a**) untreated poplar and poplar treated under (**b**) N_2, (**c**) water vapor, and (**d**) air; 1800–900 cm^{-1} section of FTIR spectra of (**e**) untreated poplar and poplar treated under (**f**) N_2, (**g**) water vapor, and (**h**) air.

3.5. Elemental Analysis

When analyzing the results from the elemental analysis, all treated samples displayed lower H/C and O/C than the untreated sample (Table 2), denoting that the thermal treatment, regardless of the specific atmosphere used, results in both the loss of oxygenated compounds and increase in unsaturations (loss of H/dehydration). Additionally, for samples treated under the vacuum at different pressures, a very clear trend of increase in the H/C ratio can be seen for increasing pressures (Table 2). That trend can be associated with processes, such as delignification and loss of aromatics, which incur in the loss of a higher amount of C in comparison to H. Since H/C increases with pressure, it can be inferred that these processes are directly dependent on oxygen concentration. It is possible that the breakdown of lignin is catalyzed by oxygen. With more extensive degradation of the lignin backbone, C can be lost in the form of CO_2 and CO, increasing H/C.

Table 2. Elemental analysis results for poplar samples treated under different pressures (200–600 hPa) and atmospheres (N_2, water vapor, and air).

Wood Sample	H/C	O/C
RAW	2.4735	1.0407
200 hPa	1.6602	0.9946
300 hPa	1.7020	0.7924
400 hPa	2.0165	0.8282
500 hPa	2.1593	0.8099
600 hPa	2.3050	0.7924
N_2	1.3219	0.5919 (0.4938) [a]
Water vapor	1.3861	0.6268
air	1.3830	0.6261 (0.5364) [a]

[a] EDS measurement.

Similarly, apart from the sample treated under 300 hPa, there is an overall decrease in O/C with increasing pressure (Table 2), indicating that a higher concentration of oxygen in the treatment atmosphere promotes a more extensive reaction/degradation of the wood sample accompanied by the loss of oxygenated compounds and leaving a higher C content with respect to O. It is very likely that a more oxidative treatment environment removes -OH (and O) groups in the form of H_2O via dehydration and condensation reactions. The polycondensation of certain byproducts can directly be responsible for repolymerization processes, gradually leading to products with lower O/C.

For the different atmospheres, following the same reasoning employed for the different pressures, an increase in H/C is expected for more oxidative atmospheres. Indeed, H/C for the sample treated under N_2 is lower than for samples treated under water vapor and air. Contrary to what was observed under reduced pressures, a slight increase in O/C is observed for samples treated under more oxidative atmospheres. In this case, it is possible that the absence of a vacuum resulted in an extended contact time between reactive oxygenated fragments initially formed and the rest of the sample, resulting in oxygen-rich, non-volatile by-products and therefore, increasing the final O/C with respect to the sample treated under the inert atmosphere. It is worth noting that very little difference has been observed in H/C and O/C between samples treated under water vapor and air. The EDS results of two selected samples treated under N_2 and air confirm the trend observed by the elemental analysis, which indicates an increase in the O/C ratio for samples treated under the more oxidative air atmosphere.

3.6. XRD

Structural changes in wood components have been assessed by means of XRD. Based on the diffractograms obtained (Figure 10), the crystallinity index of each sample has been calculated and is shown in Table 3. When poplar is treated under reduced pressure (200–500 hPa), there is very little variation of the crystallinity index with respect to the untreated samples (RAW), and there is no recognizable trend between pressure and crystallinity. Indeed, the crystallinity index for samples treated under a reduced pressure varied from 74.67% (300 hPa) to 79.07% (400 hPa). Since the crystallinity measured by XRD is directly associated with the structure of cellulose, the minimal variations observed could indicate that cellulose is minimally modified under reduced pressure due to the reduced diffusion time of by-products. When the treatment is not conducted under reduced pressure, there is a clear increase in crystallinity from 74.54% (RAW) to 78.56% (N_2) that could be attributed to an extended diffusion time of the by-products and resulting side reactions, ultimately leading to further degradation of amorphous cellulose and accounting for a higher relative concentration of crystalline cellulose. When the treatment is performed under oxidative atmospheres (water vapor and air), the increase in crystallinity is more

pronounced (80.40–80.63%), revealing that amorphous cellulose is more affected under these conditions. As mentioned previously, the samples treated under water vapor and air exhibit very similar crystallinity.

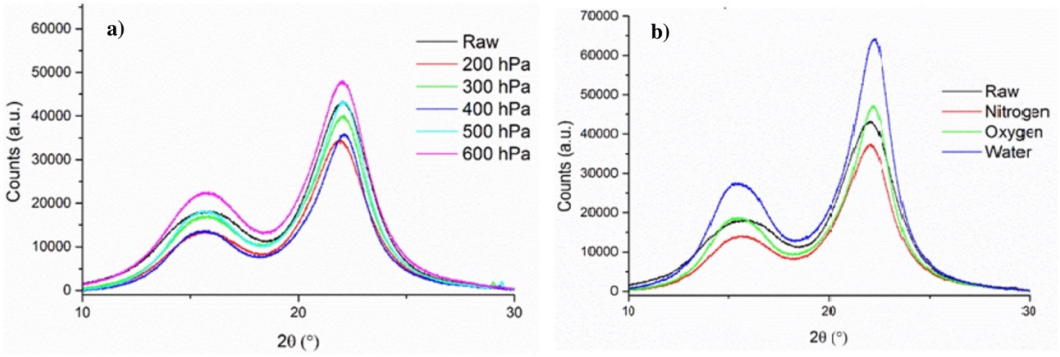

Figure 10. X-ray diffractograms of poplar samples treated under (**a**) reduced pressure and (**b**) different atmospheres.

Table 3. Calculated crystallinity index for poplar wood samples torrefied under different pressures (200 hPa to 600 hPa) and different atmospheres (N_2, water vapor, and air).

Sample	Crystallinity Index (%)
RAW	74.54
200 hPa	76.72
300 hPa	74.67
400 hPa	79.07
500 hPa	77.06
600 hPa	73.06
N_2	78.56
Water Vapor	80.63
Air	80.40

4. Conclusions

Herein, the effects of pressure and atmosphere on the torrefaction of poplar wood was elucidated. The trends observed for mass loss, color change, wood composition (via TGA/DTG analysis), functional groups (via FTIR), O/C and H/C, and XRD allowed for the interpretation of possible reaction pathways occurring during wood thermal treatment under different conditions. Changes observed under reduced pressures have been associated with the relative concentration of oxygen in the reaction atmosphere and to the reduced diffusion times experienced by reactive by-products during the treatment. Conversely, an extended diffusion time resulted in more significant changes for reactions carried out under N_2, water vapor, and air. In the absence of a vacuum, no significant difference has been observed for samples treated under water vapor and air, but more oxidative atmospheres (air and water vapor) exhibit further change/degradation in comparison to other atmosphere conditions and under the same temperature regime. Finally, the changes observed were attributed to known processes, such as dehydration, condensation, hydrolysis, and oxidation.

Author Contributions: Conceptualization, A.P.; methodology, P.R.T., A.H. and G.D.; software, A.H.; validation, R.L.Q., A.P., B.C. and M.P.; formal analysis, P.R.T., A.H., G.D., R.L.Q. and A.P.; investigation, P.R.T. and L.R.; resources, A.P. and M.P.; data curation, P.R.T., A.H. and G.D.; writing—original draft preparation, R.L.Q. and A.P.; writing—review and editing, R.L.Q.; visualization, B.C.; supervi-

sion, B.C.; project administration, B.C. and A.P.; funding acquisition, A.P. All authors have read and agreed to the published version of the manuscript.

Funding: This research was funded by the Lab of Excellence ARBRE under grant ANR-11-LABEX-0002-01, the Thomas Jefferson Fund (Embassy of France in the United States and FACE Foundation), and the National Science Foundation under grant NSF-IRES 1952402. The APC was generously waived for this submission.

Data Availability Statement: Not applicable.

Acknowledgments: The authors thank Julio Antonio Conti Silva for graciously performing the EDS analyses reported in this manuscript.

Conflicts of Interest: The authors declare no conflict of interest.

References

1. Militz, H. Heat treatment of wood: European Processes and their background. In *International Research Group Wood Preservation*; Section 4-Processes, N° IRG/WP 02-40241; International Research Group on Wood Protection: Stockholm, Sweden, 2002.
2. Korkut, S.; Korkut, D.S.; Kocaefe, D.; Elustondo, D.; Bajraktari, A.; Çakıcıer, N. Effect of thermal modification on the properties of narrow-leaved ash and chestnut. *Ind. Crops Prod.* **2012**, *35*, 287–294. [CrossRef]
3. Hakkou, M.; Pétrissans, M.; Gérardin, P.; Zoulalian, A. Investigations of the reasons for fungal durability of heat-treated beech wood. *Polym. Degrad. Stab.* **2006**, *91*, 393–397. [CrossRef]
4. Allegretti, O.; Brunetti, M.; Cuccui, I.; Ferrari, S.; Nocetti, M.; Terziev, N. Thermovacuum modification of spruce (picea abies karst.) and fir (abies albamill.) wood. *BioResources* **2012**, *7*, 3656–3669.
5. Chen, W.-H.; Lin, B.-J.; Colin, B.; Chang, J.-S.; Pétrissans, A.; Bi, X.; Pétrissans, M. Hygroscopic transformation of woody biomass torrefaction for carbon storage. *Appl. Energy* **2018**, *231*, 768–776. [CrossRef]
6. Shankar Tumuluru, J.; Sokhansanj, S.; Hess, J.R.; Wright, C.T.; Boardman, R.D. REVIEW: A Review on Biomass Torrefaction Process and Product Properties for Energy Applications. *Ind. Biotechnol.* **2011**, *7*, 384–401. [CrossRef]
7. Keeratiisariyakul, P.; Rousset, P.; Pattiya, A. Coupled effect of torrefaction and densification pre-treatment on biomass energetic and physical properties. *J. Sustain. Energy Environ.* **2019**, *10*, 1–10.
8. Kubovský, I.; Kačíková, D.; Kačík, F. Structural changes of oak wood main components caused by thermal modification. *Polymers* **2020**, *12*, 485. [CrossRef]
9. Li, M.-F.; Li, X.; Bian, J.; Xu, J.-K.; Yang, S.; Sun, R.-C. Influence of temperature on bamboo torrefaction under carbon dioxide atmosphere. *Ind. Crops Prod.* **2015**, *76*, 149–157. [CrossRef]
10. Poletto, M.; Zattera, A.J.; Santana, R.M.C. Thermal decomposition of wood: Kinetics and degradation mechanisms. *Bioresour. Technol.* **2012**, *126*, 7–12. [CrossRef]
11. Wang, S.; Dai, G.; Ru, B.; Zhao, Y.; Wang, X.; Xiao, G.; Luo, Z. Influence of torrefaction on the characteristics and pyrolysis behavior of cellulose. *Energy* **2017**, *120*, 864–871. [CrossRef]
12. Chih, Y.-K.; Chen, W.-H.; Ong, H.C.; Show, P.L. Product characteristics of torrefied wood sawdust in normal and vacuum environments. *Energies* **2019**, *12*, 3844. [CrossRef]
13. Pelaez-Samaniego, M.R.; Yadama, V.; Lowell, E.; Espinoza-Herrera, R. A review of wood thermal pretreatments to improve wood composite properties. *Wood Sci. Technol.* **2013**, *47*, 1285–1319. [CrossRef]
14. Suliman, W.; Harsh, J.B.; Abu-Lail, N.I.; Fortuna, A.-M.; Dallmeyer, I.; Garcia-Pérez, M. The role of biochar porosity and surface functionality in augmenting hydrologic properties of a sandy soil. *Sci. Total Environ.* **2017**, *574*, 139–147. [CrossRef] [PubMed]
15. Hill, C.; Altgen, M.; Rautkari, L. Thermal modification of wood—A review: Chemical changes and hygroscopicity. *J. Mater. Sci.* **2021**, *56*, 6581–6614. [CrossRef]
16. Bach, Q.-V.; Tran, K.-Q.; Skreiberg, Ø. Accelerating Wet Torrefaction Rate and Ash Removal by Carbon Dioxide Addition. *Fuel Process. Technol.* **2015**, *140*, 297–303. [CrossRef]
17. Bach, Q.-V.; Trinh, T.N.; Tran, K.-Q.; Thi, N.B.D. Pyrolysis Characteristics and Kinetics of Biomass Torrefied in Various Atmospheres. *Energy Convers. Manag.* **2017**, *141*, 72–78. [CrossRef]
18. Melkior, T.; Barthomeuf, C.; Bardet, M. Inputs of Solid-State NMR to Evaluate and Compare Thermal Reactivity of Pine and Beech Woods under Torrefaction Conditions and Modified Atmosphere. *Fuel* **2017**, *187*, 250–260. [CrossRef]
19. Nakason, K.; Khemthong, P.; Kraithong, W.; Chukaew, P.; Panyapinyopol, B.; Kitkaew, D.; Pavasant, P. Upgrading Properties of Biochar Fuel Derived from Cassava Rhizome via Torrefaction: Effect of Sweeping Gas Atmospheres and Its Economic Feasibility. *Case Stud. Therm. Eng.* **2021**, *23*, 100823. [CrossRef]
20. Nguyen, Q.; Nguyen, D.D.; He, C.; Bach, Q.-V. Pretreatment of Korean Pine (*Pinus koraiensis*) via Wet Torrefaction in Inert and Oxidative Atmospheres. *Fuel* **2021**, *291*, 119616. [CrossRef]
21. Rousset, P.; Macedo, L.; Commandré, J.-M.; Moreira, A. Biomass Torrefaction under Different Oxygen Concentrations and Its Effect on the Composition of the Solid By-Product. *J. Anal. Appl. Pyrolysis* **2012**, *96*, 86–91. [CrossRef]
22. Saadon, S.; Uemura, Y.; Mansor, N. Torrefaction in the Presence of Oxygen and Carbon Dioxide: The Effect on Yield of Oil Palm Kernel Shell. *Procedia Chem.* **2014**, *9*, 194–201. [CrossRef]

23. Li, R.; Wu, C.; Zhu, L.; Hu, Z.; Xu, J.; Yang, Y.; Yang, F.; Ma, Z. Regulation of the Elemental Distribution in Biomass by the Torrefaction Pretreatment Using Different Atmospheres and Its Influence on the Subsequent Pyrolysis Behaviors. *Fuel Process. Technol.* **2021**, *222*, 106983. [CrossRef]
24. Brachi, P.; Chirone, R.; Miccio, M.; Ruoppolo, G. Fluidized Bed Torrefaction of Biomass Pellets: A Comparison between Oxidative and Inert Atmosphere. *Powder Technol.* **2019**, *357*, 97–107. [CrossRef]
25. Ramos-Carmona, S.; Delgado-Balcázar, S.; Perez, J.F. Physicochemical Characterization of Torrefied Wood Biomass under Air as Oxidizing Atmosphere. *BioResources* **2017**, *12*, 5428–5448. [CrossRef]
26. Chen, W.-H.; Lu, K.-M.; Lee, W.-J.; Liu, S.-H.; Lin, T.-C. Non-Oxidative and Oxidative Torrefaction Characterization and SEM Observations of Fibrous and Ligneous Biomass. *Appl. Energy* **2014**, *114*, 104–113. [CrossRef]
27. Sun, Y.; Sun, Y.; Chen, W.; Wang, S.; Liang, G.; Li, W.; Ma, Z.; Zhang, W. Effect of Torrefaction Temperature and O_2 Concentration on the Pyrolysis Behaviour of Moso Bamboo. *BioResources* **2020**, *15*, 6344–6370. [CrossRef]
28. González Martínez, M.; Hélias, E.; Ratel, G.; Thiéry, S.; Melkior, T. Torrefaction of Woody and Agricultural Biomass: Influence of the Presence of Water Vapor in the Gaseous Atmosphere. *Processes* **2020**, *9*, 30. [CrossRef]
29. Lee, Y.; Yang, W.; Chae, T.; Kang, B.; Park, J.; Ryu, C. Comparative Characterization of a Torrefied Wood Pellet under Steam and Nitrogen Atmospheres. *Energy Fuels* **2018**, *32*, 5109–5114. [CrossRef]
30. Chen, W.-H.; Lu, K.-M.; Liu, S.-H.; Tsai, C.-M.; Lee, W.-J.; Lin, T.-C. Biomass Torrefaction Characteristics in Inert and Oxidative Atmospheres at Various Superficial Velocities. *Bioresour. Technol.* **2013**, *146*, 152–160. [CrossRef]
31. Esteves, B.M.; Pereira, H.M. Wood modification by heat treatment: A review. *BioResources* **2009**, *4*, 370–404. [CrossRef]
32. Pétrissans, A.; Younsi, R.; Chaouch, M.; Gérardin, P.; Pétrissans, M. Wood Thermodegradation: Experimental Analysis and Modeling of Mass Loss Kinetics. *Maderas Cienc. Tecnol.* **2014**, *16*, 133–148. [CrossRef]
33. Tooyserkani, Z.; Sokhansanj, S.; Bi, X.; Lim, J.; Lau, A.; Saddler, J.; Kumar, L.; Lam, P.S.; Melin, S. Steam Treatment of Four Softwood Species and Bark to Produce Torrefied Wood. *Appl. Energy* **2013**, *103*, 514–521. [CrossRef]
34. Chaouch, M.; Candelier, K.; Dumarçay, S.; Pétrissans, A.; Pétrissans, M.; Gérardin, P. Development of a Quality Control Assessment Method to Predict Properties of Heat Treated Wood. In Proceedings of the IRG/WP-IUFRO, Estoril, Portugal, 8–13 July 2012.
35. Candelier, K.; Dumarçay, S.; Pétrissans, A.; Gérardin, P.; Pétrissans, M. Mechanical Properties of Heat Treated Wood after Thermodegradation under Different Treatment Intensity. In Proceedings of the 1st International Congress, Cost Action FP0904, Biel, Switzerland, 16–18 February 2011.
36. Rosu, D.; Teaca, C.-A.; Bodirlau, R.; Rosu, L. FTIR and Color Change of the Modified Wood as a Result of Artificial Light Irradiation. *J. Photochem. Photobiol. B Biol.* **2010**, *99*, 144–149. [CrossRef]
37. Xi, Y.; Yuan, X.; Tan, M.; Jiang, S.; Wang, Z.; Huang, Z.; Wang, H.; Jiang, L.; Li, H. Properties of Oxidatively Torrefied Chinese Fir Residue: Color Dimension, Pyrolysis Kinetics, and Storage Behavior. *Fuel Process. Technol.* **2021**, *213*, 106663. [CrossRef]
38. Sivrikaya, H.; Tesařová, D.; Jeřábková, E.; Can, A. Color Change and Emission of Volatile Organic Compounds from Scots Pine Exposed to Heat and Vacuum-Heat Treatment. *J. Build. Eng.* **2019**, *26*, 100918. [CrossRef]
39. Sun, S.-N.; Li, H.-Y.; Cao, X.-F.; Xu, F.; Sun, R.-C. Structural Variation of Eucalyptus Lignin in a Combination of Hydrothermal and Alkali Treatments. *Bioresour. Technol.* **2015**, *176*, 296–299. [CrossRef]
40. Colin, B.; Quirino, R.L.; Ntsika-Mbou, C.Y.; Lin, Y.-Y.; Lin, B.-J.; Leconte, F.; Petrissans, A.; Chen, W.-H.; Petrissans, M. Behavior of Wood during the Thermal Transition between Torrefaction and Pyrolysis: Chemical and Physical Modifications. *Wood Mater. Sci. Eng.* **2021**, 1–10. [CrossRef]
41. Safar, M.; Lin, B.-J.; Chen, W.-H.; Langauer, D.; Chang, J.-S.; Raclavska, H.; Pétrissans, A.; Rousset, P.; Pétrissans, M. Catalytic Effects of Potassium on Biomass Pyrolysis, Combustion and Torrefaction. *Appl. Energy* **2019**, *235*, 346–355. [CrossRef]
42. Li, Y.; Khanal, S.K. (Eds.) *Bioenergy: Principles and Applications*; Wiley Blackwell: Hoboken, NJ, USA, 2017.
43. Zhang, B.; Petrissans, M.; Petrissans, A.; Pizzi, A.; Colin, B. Furanic Polymerization Causes the Change, Conservation and Recovery of Thermally-Treated Wood Hydrophobicity before and after Moist Conditions Exposure. *Polymers* **2022**, *15*, 221. [CrossRef]
44. Popescu, M.-C.; Froidevaux, J.; Navi, P.; Popescu, C.-M. Structural Modifications of Tilia Cordata Wood during Heat Treatment Investigated by FT-IR and 2D IR Correlation Spectroscopy. *J. Mol. Struct.* **2013**, *1033*, 176–186. [CrossRef]
45. Nishiyama, Y.; Sugiyama, J.; Chanzy, H.; Langan, P. Crystal Structure and Hydrogen Bonding System in Cellulose I α from Synchrotron X-Ray and Neutron Fiber Diffraction. *J. Am. Chem. Soc.* **2003**, *125*, 14300–14306. [CrossRef] [PubMed]
46. Li, M.-Y.; Cheng, S.-C.; Li, D.; Wang, S.-N.; Huang, A.-M.; Sun, S.-Q. Structural Characterization of Steam-Heat Treated Tectona Grandis Wood Analyzed by FT-IR and 2D-IR Correlation Spectroscopy. *Chin. Chem. Lett.* **2015**, *26*, 221–225. [CrossRef]
47. Popescu, C.-M.; Popescu, M.-C.; Vasile, C. Characterization of Fungal Degraded Lime Wood by FT-IR and 2D IR Correlation Spectroscopy. *Microchem. J.* **2010**, *95*, 377–387. [CrossRef]
48. Özgenç, Ö.; Durmaz, S.; Boyaci, I.H.; Eksi-Kocak, H. Determination of Chemical Changes in Heat-Treated Wood Using ATR-FTIR and FT Raman Spectrometry. *Spectrochim. Acta Part A Mol. Biomol. Spectrosc.* **2017**, *171*, 395–400. [CrossRef] [PubMed]
49. Popescu, C.; Jones, D.; Kržišnik, D.; Humar, M. Determination of the Effectiveness of a Combined Thermal/Chemical Wood Modification by the Use of FT–IR Spectroscopy and Chemometric Methods. *J. Mol. Struct.* **2020**, *1200*, 127133. [CrossRef]

50. Robles, E.; Herrera, R.; De Hoyos Martínez, P.L.; Fernández Rodríguez, J.; Labidi, J. Valorization of Heat-Treated Wood after Service Life through a Cascading Process for the Production of Lignocellulosic Derivatives. *Resour. Conserv. Recycl.* **2021**, *170*, 105602. [CrossRef]
51. Gu, X.; Liu, C.; Jiang, X.; Ma, X.; Li, L.; Cheng, K.; Li, Z. Thermal Behavior and Kinetics of the Pyrolysis of the Raw/Steam Exploded Poplar Wood Sawdust. *J. Anal. Appl. Pyrolysis* **2014**, *106*, 177–186. [CrossRef]